Materials Letters 64 (2010) 2502–2504

Contents lists available at ScienceDirect

Materials Letters

journal homepage: www.elsevier.com/locate/matlet

Fabrication of bismuth oxide–tin oxide nanowires by direct thermal oxidation of Bi–Sn eutectic nanowires

Shih-Hsun Chen [a], Chiu-Yen Wang [b], Tzeng-Feng Liu [a], Chuen-Guang Chao [a,*]

[a] Department of Materials Science and Engineering, National Chiao Tung University, Hsinchu 30050, Taiwan
[b] Department of Materials Science and Engineering, National Tsing Hua University, Hsinchu 30013, Taiwan

ARTICLE INFO

Article history:
Received 26 July 2010
Accepted 6 August 2010
Available online 19 August 2010

Keywords:
Thermal oxidation
Bi–Sn eutectic nanowires
BiO_x–SnO_x nanowires

ABSTRACT

Bismuth oxide–tin oxide (BiO_x–SnO_x) heterostructure nanowires with a diameter of 70 nm were fabricated by directly annealing Bi–Sn eutectic nanowires synthesized by the vacuum hydraulic pressure injection process. After removal of AAO (Anodic Aluminum Oxide) template with an etching solution, a spontaneous oxide was formed on nanowires to enclose the Bi–Sn eutectic alloys. While these nanowires went through the annealing process with the proper heating rate of 50 °C/min, the well-annealed oxide nanowires remain solid, straight and segmental. The results of cathodoluminescence (CL) spectrum and photoresponse proved that the products consisted of bismuth oxide and tin oxide. This fabrication methodology provides a simple way to produce one-dimensional oxide nanomaterials.

1. Introduction

Functional metal oxides are used in many applications due to their unique physical properties. Among them, tin oxide (SnO_2) and bismuth oxide (Bi_2O_3) are two important strategic materials in modern solid-state technology. As semiconductors with large and wide energy band gaps, they are widely applied to gas sensors [1,2], optoelectronic devices [3,4], photovoltaic cells [5,6], and transparent conduction electrodes [7]. However, it is generally accepted that the chemical and physical properties of these materials are influenced by their dimensions. One-dimensional materials, such as nanowires, nanorods and nanotubes, are considered ideal materials for both fundamental and applied research.

Due to the scientific and technological importance of SnO_2 and Bi_2O_3, many studies have published synthesis reports on their one-dimensional nanostructures. Chemical vapor deposition (CVD) [8,9], chemical method [10,11], laser ablation [12], and thermal evaporation [13] are common bottom-up approaches to the preparation of one-dimensional self-assembly materials in the literature. Even so, to seek a simpler, cheaper, and more stable process is always the top objective for industrial applications.

In this study, we present a fabrication method to obtain BiO_x–SnO_x nanowires by directly oxidizing Bi–Sn eutectic nanowires in an air furnace. The Bi–Sn eutectic nanowires are of a segmental microstructure, and are synthesized by a template-assisted casting process [14]. The as-injected nanowires have a regular structure; thus, the BiO_x–SnO_x nanowires are simultaneously obtained through a thermal oxidation process; and retain the segmental microstructure. The optical properties are evaluated as the evidence for both oxides.

2. Experimental procedures

The segmental Bi–Sn eutectic nanowires were synthesized by the vacuum hydraulic pressure injection process [14]; the as-injected nanowires had an average diameter of 70 nm and lengths of several microns. Details of the injection process have been reported previously [15,16].The prepared materials were put into an air furnace and directly annealed at 700 °C for 1 h. After cooling to room temperature, the BiO_x–SnO_x nanowires were obtained.

The morphology and appearance of metal and oxide nanowires were characterized by field-emission scanning electron microscopy (FESEM, JSM-6500) and transmission electron microscopy (TEM, JEM-2010) combined with energy-dispersive X-ray spectrometry (EDS).

Spectroscopy of the oxide nanowires was performed by SEM-cathodoluminescence (CL) at room temperature with a commercial Gatan MonoCL2 system using an alkali halide photomultiplier detector attached to the SEM described above. To characterize the photocurrent, an ultraviolet (UV) lamp ($\lambda = 325$ nm) was used as a light source; the power density of the light was 10 mW/cm^2. The photocurrent was measured by a two-probe I–V system using a Keithley 237 source measurement unit.

3. Results and discussion

The nanostructure materials synthesized by this injection process formed an oxide shell during the removal of the AAO template. This

* Corresponding author.
E-mail address: cgchao@mail.nctu.edu.tw (C.-G. Chao).

0167-577X/$ – see front matter © 2010 Elsevier B.V. All rights reserved.
doi:10.1016/j.matlet.2010.08.034

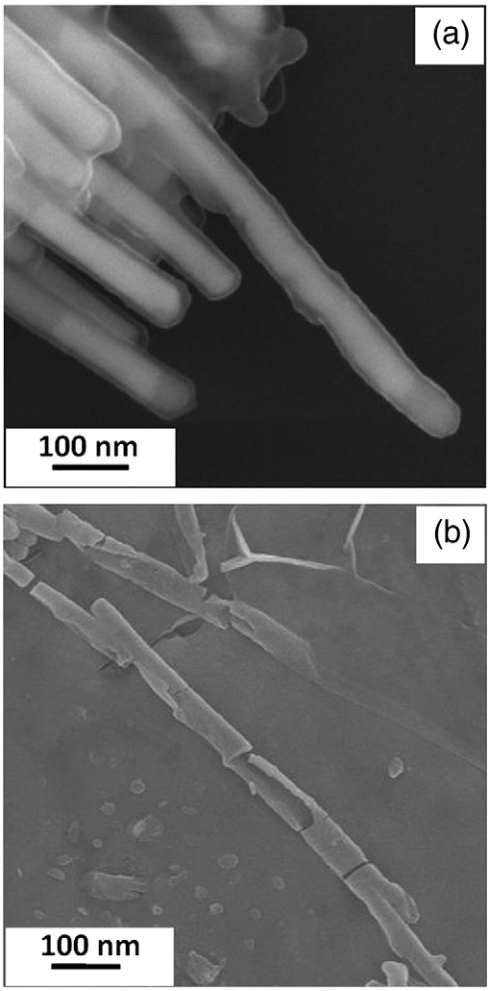

Fig. 1. (a) SEM image of as-injected Bi–Sn eutectic nanowires after removal of the AAO template with an etching solution. The core–shell of the segmental structure can be observed. (b) SEM image of nanowires annealed with an excessive heating rate.

spontaneous oxide shell was stable and served as a container to preserve the alloys inside during the annealing process [17]. To prevent the metastable phase, the annealing temperature must be no higher than 729 °C [18]; thus, the temperature was 700 °C.

Fig. 1(a) shows an SEM image of as-injected Bi–Sn nanowires after removal of the AAO template with an etching solution (0.4 M H_3PO_4 + 0.2 M CrO_3) at 60 °C for 2 h and washing with ethanol and deionized water. A thin oxide layer could be observed on the products. These spontaneous oxides formed a core–shell structure and enclosed the alloys within the nanowires for the next annealing treatment. However, the initial oxides were not dense enough for rapid expansion of liquid alloys. If the heating rate was higher than 100 °C/min, the alloys would not convert to oxides within the shell and would instead leak out of it. In Fig. 1(b), the SEM image shows the residual oxide shells after annealing with an excessive heating rate. The fragmentation of the annealed wires under fast heating was mainly caused by the brittleness of initial oxides. The original oxide on bismuth segments was thicker and incomplete [16]. Upon subsequent annealing, liquid alloys leak out the oxide shell from locations such as defects and interfaces, which results in a broken segmental structure.

Fig. 2 shows TEM images of annealed nanowires at the excessive and proper conditions respectively. In Fig. 2(a), most alloys leaked out, and only fractured oxide nanowires were obtained after the excessive annealing process. Moreover, some complete segmental oxide nanowires could be still discovered. This was due to the remaining AAO, which served as dense oxide shells of Bi–Sn nanowires and restrained the alloys from leaking. As the heating rate was reduced to a proper value of 50 °C/min, the morphology of oxide nanowires revealed a solid rod with a segmental structure, as shown in Fig. 2(b). The differences in the segments originally resulted from precipitation of bismuth and tin in sequence. Thus, the oxide nanowires followed the array of Bi–Sn eutectic nanowires.

While Bi–Sn eutectic nanowires were annealed at 700 °C for 1 h with a heating rate of 50 °C/min, the one-dimensional nano-compounds made of bismuth oxide and tin oxide were produced in the shape of straight wires. The TEM image in Fig. 3(a) shows that the morphology of well-annealed nanowires retained the segmental structure. Furthermore, compositions of nanowires were also determined by EDS analysis, presented in Fig. 3(b). The observation indicates that BiO_x–SnO_x nanowires were successfully produced through the annealing process. The Mo and Ta peaks came from the TEM grid and heating holder, respectively.

To ensure the types of oxide nanowires, an SEM-CL spectrum was utilized to inspect the radiative property of oxides at room temperature. In Fig. 4, the pulsating line, spreading from 200 nm to 800 nm, represents the raw CL spectrum of oxide nanowires, and its fitting curve is also shown. According to previous studies [8,13,19], it could be decomposed into two sub-curves. One is sharper and ranges from 300 nm to 530 nm. Leonite [13] reported that the absorption curve of the Bi–O system mainly resulted from the band gaps of α-Bi_2O_3 and Bi_2O_3 (E_g = 2.29–3.31 eV). The other is consistent

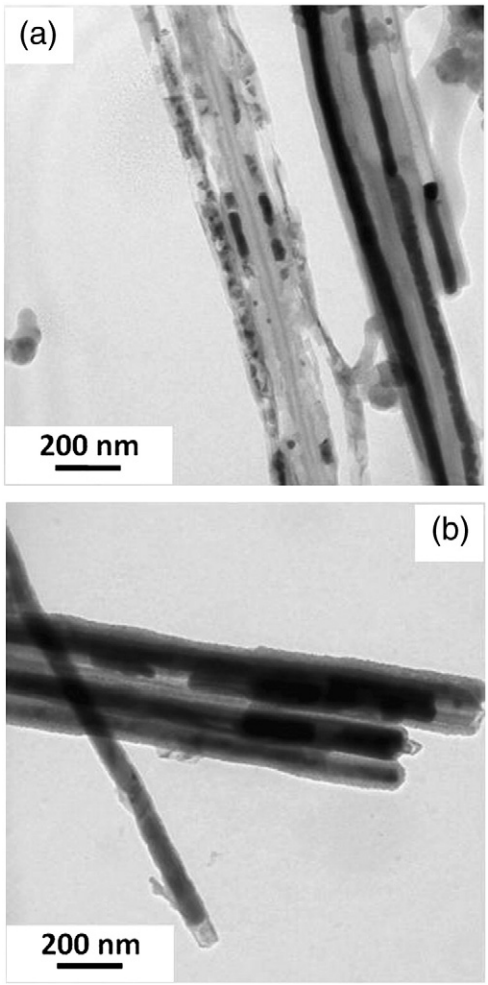

Fig. 2. TEM images of annealed Bi–Sn eutectic nanowires under (a) excessive and (b) proper heating rates. The oxides were not dense enough to confine the melting alloys under an excessive heating rate, or the proper annealing condition could result in stiff and complete nanowires. The residual AAO would help to maintain the integrity of melting alloys.

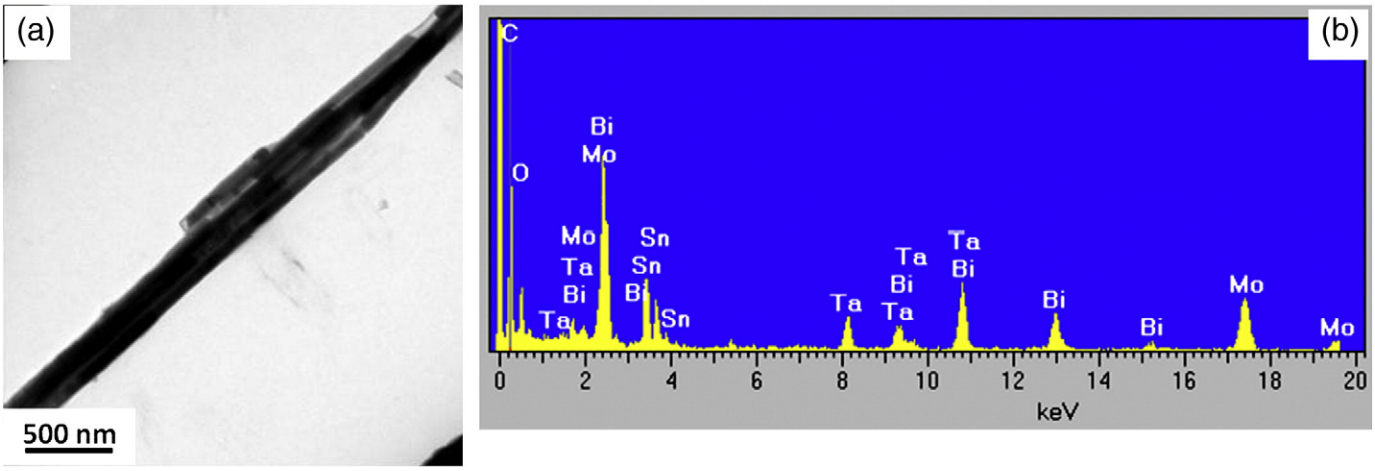

Fig. 3. (a) TEM image of well-annealed Bi–Sn eutectic nanowires. (b) EDS was used to identify the composition of nanowires. The Mo and Ta peaks came from the TEM grid and heating holder, respectively.

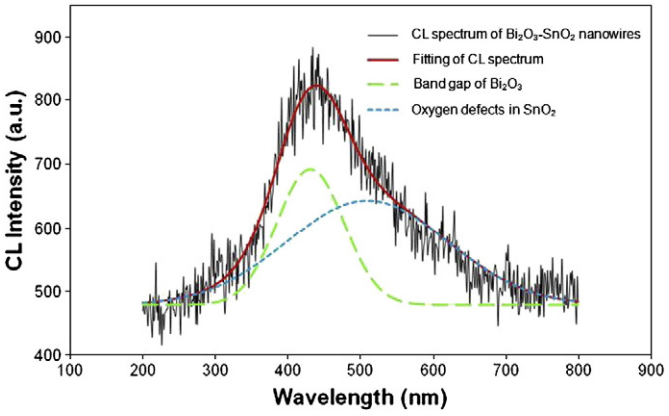

Fig. 4. CL spectrum from BiO_x–SnO_x nanowires with an average diameter of 70 nm. The curve was composed of two emission resources: the band gap of Bi_2O_3 and the oxygen vacancies in SnO_2 [8,13,19].

with the hypothesis that the transition is due to deep levels in the band gap due to surface states induced by oxygen vacancies of SnO_2 nanowire, presented by the authors [8,19]. Thus, the CL spectrum clarifies the types of oxides and supports the existence of BiO_x–SnO_x nanowires.

Fig. 5 shows the photoresponse of BiO_x–SnO_x nanowires at a bias voltage of 0.8 V in air under modulated illumination of 325 nm wavelength light. The photocurrent of the oxide nanowires was

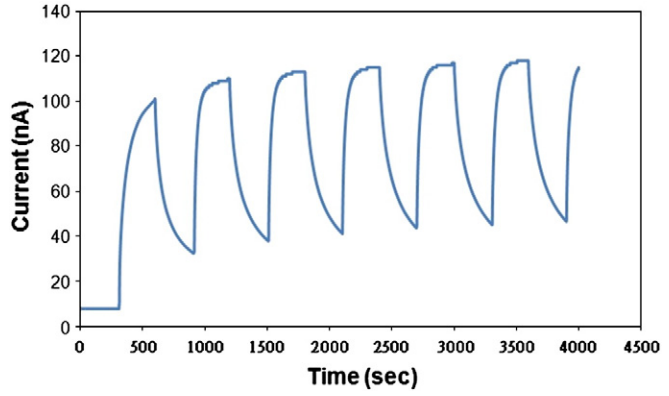

Fig. 5. Photoresponse of Bi_2O_3–SnO_2 nanotubes with periodic irradiation of light under continuous illumination of 325 nm in air at a bias voltage of 0.8 V.

increased rapidly when the light was switched on, and it saturated. After the light was switched off, the current decayed to one-tenth of the saturated value within 300 s. This phenomenon indicated that the photoresponse of n-type oxide semiconductor is controlled by surface effects, such as oxygen absorption under dark conditions by trapping electrons ($O^2{}_{(g)} + e^- = O_2{}^-{}_{(ad)}$) and photodesorption of oxygen ion by capturing photogenerated holes ($h^+ + O_2{}^-{}_{(ad)} = O_{2(g)}$) [20,21]. Recent studies [22,23] have also focused on functional oxides; and identified them with this optical mechanism.

4. Conclusions

This work demonstrates that the compound nanowires of bismuth oxide and tin oxide were produced by directly annealing Bi–Sn eutectic nanowires synthesized by the vacuum hydraulic pressure injection process. The well-annealed oxide nanowires were straight and solid, and retained the segmental structure. Moreover, the CL spectrum and photoresponse analyses confirmed that the types of oxides were BiO_x–SnO_x nanowires. The characteristics of this fabrication methodology provide a simple way to produce one-dimensional oxide nanomaterials.

References

[1] Khanna A, Kumar R, Bhatti SS. Appl Phys Lett 2003;82:4388–90.
[2] Kanazawa E, Sakai G, Shimanoe K, Kanmura Y, Teraoka Y, Miura N, et al. Sens Actuators B 2001;77:72–7.
[3] Tatsuyama C, Ichimura S. Jpn J Appl Phys 1976;15:843-794.
[4] Leontie L, Caraman M, Visinoiu A, Rusu GI. Thin Solid Films 2005;473:230–5.
[5] Turrion M, Bisquert J, Salvador P. J Phys Chem B 2003;107:9397–403.
[6] George J, Pradeep B, Joseph KS. Phys Status Solidi A 1987;100:513–9.
[7] He YS, Campbell JC, Murphy RC, Arendt MF, Swinnea JS. J Mater Res 1993;8:3131–4.
[8] Calestani D, Zha M, Zappettini A, Lazzarini L, Salviati G, Zanotti L, et al. Mater Sci Eng C 2005;25:625–30.
[9] Kim HW, Myung JH, Shim SH. Solid State Commun 2006;137:196–8.
[10] Gujar TP, Shinde VR, Lokhande CD, Han SH. Mater Sci Eng B 2006;133:177–80.
[11] Kolmakov A, Zhang Y, Cheng G, Moskovits M. Adv Mater 2003;15:997–1000.
[12] Liu Z, Zhang D, Han S, Li C, Tang T, Jin W, et al. Adv Mater 2003;15:1754–7.
[13] Leontie L, Caraman M, Alexe M, Harnagea C. Surf Sci 2002;507–10:480–5.
[14] Chen SH, Chen CC, Luo ZP, Chao CG. Mater Lett 2009;63:1165–8.
[15] Chen CC, Kuo CG, Chen JH, Chao CG. Jpn J Appl Phys 2004;43:8354–9.
[16] Chen SH, Wang CY, Chen LJ, Liu TF, Chao CG. J Nanosci Nanotechnol 2010;10:1–8.
[17] Kolmakov A, Zhang Y, Moskovits M. Nano Lett 2003;3:1125–9.
[18] Li L, Yang YW, Li GH, Zhang LD. Small 2006;2:548–53.
[19] Prades JD, Arbiol J, Cirera A, Morante JR, Avella M, Zanotti L, et al. Sens Actuators B 2007;126:6–12.
[20] Melnick DA. J Chem Phys 1957;26:1136–46.
[21] Keezer R. J Appl Phys 1961;35:1866–7.
[22] Lee JS, Sim SK, Min B, Cho K, Kim SW, Kim S. J Cryst Growth 2004;267:145–9.
[23] Wang Y, Ramos I, Santiago-Aviles JJ. J Appl Phys 2007;102:093517.